Heliyon 10 (2024) e29287

Contents lists available at ScienceDirect

Heliyon

journal homepage: www.cell.com/heliyon

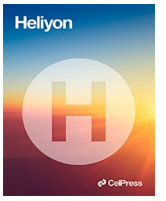

Research article

Exploring the optical properties of metal-modified melanin following ultraviolet irradiation: An experimental and theoretical study using density functional theory

Nawal Madkhali *, Saja Algessair

Physics Department, College of Science, Imam Mohammad Ibn Saud Islamic University (IMSIU), Riyadh, 13318, Saudi Arabia

ARTICLE INFO

Keywords:
Eumelanin
Absorption properties
UV region
Transition metals
Nigella sativa

ABSTRACT

Melanin has an important function to protect humans from sunlight because of its broad spectrum of light absorption. This characteristic varies according to the nature of absorption and the amount of melanin manufactured. This study focused on UV–Vis absorption of melanin doped with (Fe, Co, Zn) ions. According to the result, eumelanin exhibits substantial absorption in a broad range between (200–500 nm) corresponding to the extension of the violet to the visible region. In the theoretical section of the results, using density functional theory (DFT) revealed an improvement in the optical reactivity properties of transition metals eumelanin. The presence of transition metals led to semiconductor-like behavior and optical reactivity regions in the energy range of 4.4–4.6 electron volts, clearly indicating enhanced structural properties in the presence of metals. In this study, we aspire to investigate the ability to modify the absorption properties of eumelanin can effectively contribute to the treatment of some skin diseases caused by excessive eumelanin secretion.

1. Introduction

Eumelanin is a natural pigment found in most organisms [1]. It can be considered the main responsible of the color of hair and skin [2]. Eumelanin has a broad band absorption spectrum from ultraviolet to visible range [3]. Because of this property, eumelanin works as an efficient photo protective pigment. As a result of the uncertainty that scientists continue to be puzzled by the nature of the electronic structure of melanin and how the eumelanin aggregate, therefore it is difficult to understand the absorption spectrum of eumelanin which increasing monotonically at high energy. Based on these properties of eumelanin, it is important to study its electronic structure and its optical properties. According to many experimental measurements in X-ray diffraction and scanning tunneling microscopy for synthetic and natural eumelanin, the size of order 145-20 nm is the pentamers and/or tetramers formed by DHI monomer were the most molecular structures of eumelanin [4]. Because eumelanin polymers have unique light-absorbing properties and have no bottom terminal edge compared to other organic compounds. Eumelanin (black melanin) is mainly composed of oligomers of 5,6-dihydroxyindole (DHI) and 5,6-dihydroxyindole-2-carboxylic acid (DHICA), while pheomelanin (orange-red Melanin) is derived from benzothiazine units. Neuromelanin, distinct from these two types of melanin, is thought to be a complex of dihydroxyindole and benzothiazine units [5–7] One of melanin's most crucial biological roles is metal chelation. Melanin's ability to bind to reactive metal ions reduces the body's exposure to oxidative stress [8]. Where metals are organizing in metabolism with the

* Corresponding author.
E-mail address: namadkhali@imamu.edu.sa (N. Madkhali).

https://doi.org/10.1016/j.heliyon.2024.e29287
Received 8 November 2023; Received in revised form 3 April 2024; Accepted 4 April 2024
Available online 4 April 2024

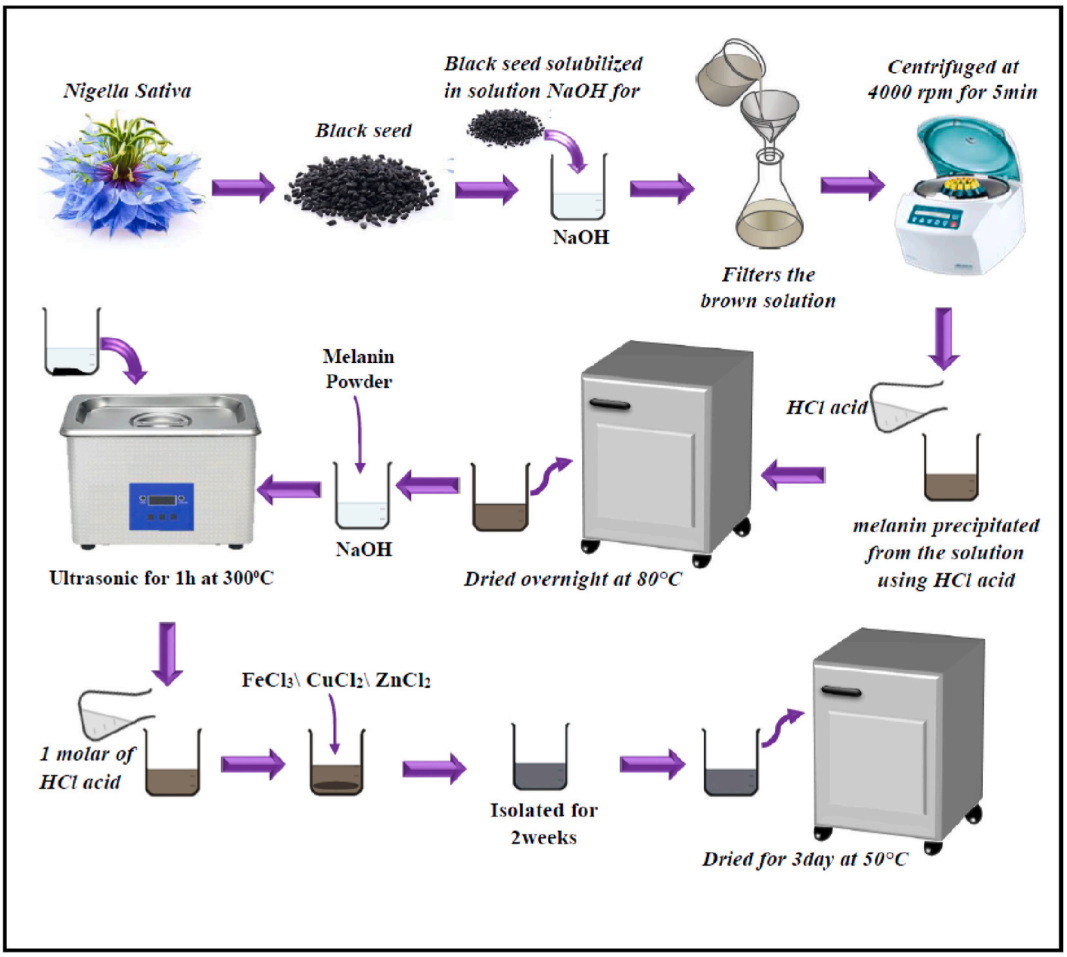

Fig. 1. Schematic of the process followed for the synthesis of eumelanin doped with metal ions.

participation of melanin that works specifically as an effective antioxidant [4,9]. The functional groups associated with the molecular of melanin are central to the metal coordinating abilities exhibited by melanin. It should be noted that it can summarize the role of eumelanin in the gouge minerals in the two main points: Melanin has a high affinity for Ca (II) or Zn (II), up to 1.5–1.6 mmol/g. Melanin acts as a reservoir for these metals and releases them under specific circumstances. However, by catalyzing Fenton reactions, heavier metal cations like Fe (III) and Cu (II) can harm biological systems. Melanin binds to these metals, preventing cellular components from reducing them and causing oxidative stress in the process. Several academics [10,11] are reported the binding capacity of natural melanin to heavy transition metals (TMs) such as magnesium, iron and copper was determined using inductively coupled plasma mass spectrometry. These TMs can interact with the COOH group in melanin to form bonds and exchange ions. It is worth pointing out; that the binding ability for TMs metals used to figure out the amount of DHICA in melanin [9,12]. The decreased binding ability with age suggests that the numbers of functional groups such as (carboxyl group) or DHICA monomers decreases and less efficient as an antioxidant. It is worth noting: that melanin bind to TMs metal ions by two main types of binding sites: The first is strong reacting sites with the association constant Ka: 10^4–10^6 M^{-1} and the other is weak reacting ones with Ka = 10^3 M^{-1} [13]. Such a mechanism in connection with transition metals has been attributed with explaining the electrical and electronic properties of melanin.

Recently, several studies have revealed new applications of melanin in the medical field due to its properties: such as redox behavior, UV wide absorption, high biocompatibility, chelating ability and antitumor effects. Moreover, Intraneuronal melanin may serve as a protective factor for cells against toxins, oxidative stress, and metals [14]. Lately,- Obida [15] showed that the HM from Nigella sativa (L.) black seed coats stimulated the TLR4/COX-2 pathway in human gastric epithelial cells, increasing the release of PGE2 and IL-6 [15].

Overall, the reduction of the amorphous structure of melanin by metal oxides is a complex process that involves electron transfer, oxidation-reduction reactions, and alterations to the molecular arrangement of melanin. Ongoing research aims to fully comprehend the underlying mechanisms of this phenomenon and explore its potential applications in various fields, including materials science and biomedicine.

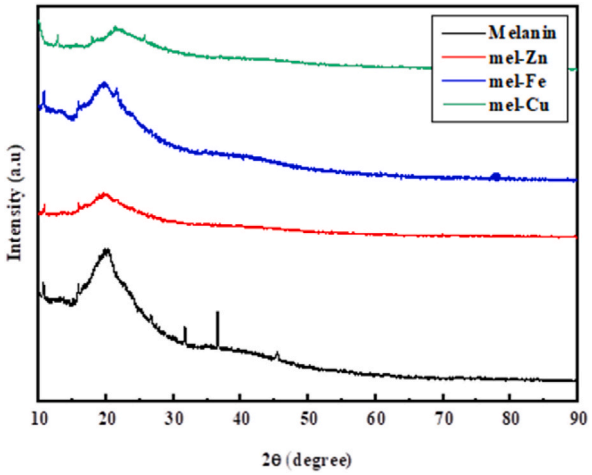

Fig. 2. XRD patterns of the pure natural eumelanin, mel-Zn, mel-Fe and mel-Cu.

The aim of the present study, to investigate extensive optical study on both:the experimental and theoretical sides of eumelanin after interacting with Fe, Zn and Cu ions. These TMs atoms can induce the intrinsic properties of eumelanin, making them potential candidates for biological applications for the treatment of skin diseases caused by increased eumelanin secretion.

2. Sample preparation

Eumelanin was extract from (*Nigella Sativa*) as reported in Ref. [16]. First, the herbal eumelanin was prepared by its extraction from black seed. After the addition of sodium hydroxide (1 Molar) to 5 g of herbal eumelanin, the ultrasound device is used to sonicate the particles of the system for 1 h at a temperature of 300 °C. Then, adding hydrochloric acid (1 M) to the solution to reach the normal pH. For the synthesis of Fe ions doped with eumelanin (Fe-Mel), we add the metal salt solvent Iron (II) chloride ($FeCl_3$) in ratio 1: 20 to eumelanin solution. The mixtures were isolated for two weeks, and the changes in the colors of the solutions were observed. The samples were washed and dried in the oven for three days at a temperature of 50 °C. The same steps were repeated for preparing samples of Cu ions doped with eumelanin (Cu-Mel) and Zn ions doped with eumelanin (Zn-Mel) using $CuCl_2$ and $ZnCl_2$, respectively. The process followed for the synthesis of our samples illustrated in Fig. 1. 1. Hydrochloric acid, Sodium hydroxide, Copper(II) chloride, Cobalet chloride and Iron(II)chloride were provided by Sigma Aldrich. Deionized water (resistivity 18.0 M Ω cm) was used for the preparation of all solutions. We described the purity and the preparation methods in more detail in our previous work reported in Ref. [17].

2.1. Characterization techniques

In order to measure the X-ray diffraction (XRD) patterns for our samples, a Bruker D8 Discover diffractometer with Cu-Kα radiation of $\lambda = 1.5406$ Å was used. A PerkinElmer 580 B-IR spectrometer was used to obtain Fourier transform infrared (FTIR) spectra. A PerkinElmer Lambda 40 spectrophotometer was used to measure the UV–vis absorption spectra in the 200–800 nm region. Through JEM – 2100 F- JEOL Ltd, from the field emission electron microscope (FE-TEM) images were obtained.

2.2. Computational methods

Our work involves conducting theoretical simulations using the FP-LAPW + lo technique, an all-electron method that relies on density functional theory (DFT) for accurate calculations. To perform these simulations, we utilize the WEN2K Simulation Package, which provides powerful tools for analyzing and predicting material properties.In our calculations, we take into account the exchange-correlation potential within the spin generalized gradient approximation (σ-GGA). This choice allows us to accurately describe the electronic interactions in the system under investigation. Specifically, when dealing with systems that contain 3d-transition metals, it becomes crucial to incorporate spin-polarized calculations. This is necessary to capture the intricate interplay between the partially occupied 3D orbitals of the transition metal atoms and the organic components within the system.To determine the key properties related to the structure, electronic behavior, and optical characteristics of both pure DHICA and TMs-DHICA systems (where TMs represent the transition metals Fe, Cu, and Zn), we adopt a computational setup where the isolated monomers are placed within a cubic simulation box. This box has dimensions of 20 Å × 20 Å x 20 Å, providing sufficient space for the monomers to interact and explore their structural and electronic configurations. By employing this comprehensive approach, our objective is to gain insights into the influence of transition metals on the structural, electronic, and optical properties of DHICA-based systems. This investigation will contribute to a better understanding of these systems and potentially guide the design of novel functional materials.

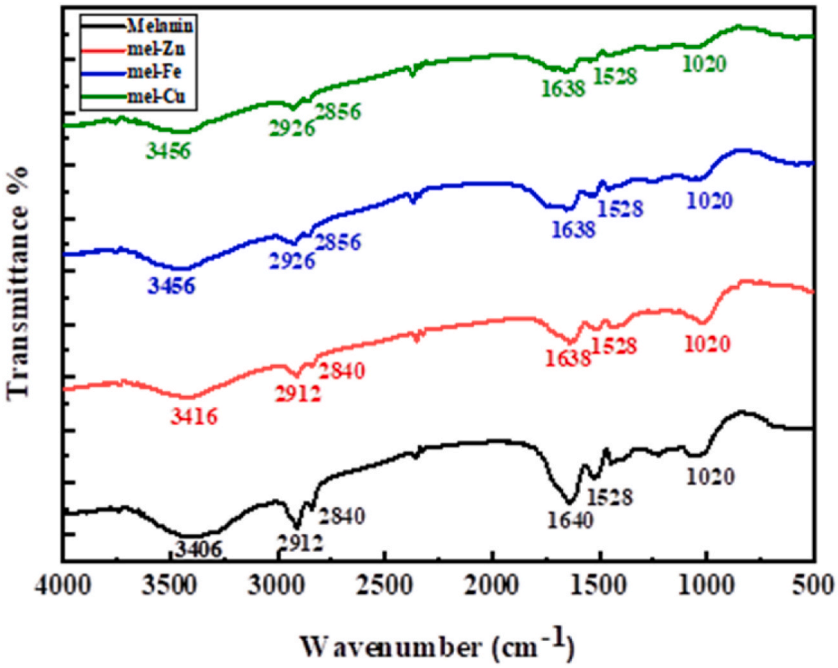

Fig. 3. The FTIR spectra for pure natural eumelanin, mel-Zn, mel-Fe and mel-Cu.

2.3. X-ray diffraction (XRD)

The XRD patterns of the pure natural eumelanin and the one doped with Zn, Fe and Cu ions are depicted in Fig. 2. The XRD patterns show that all our samples have amorphous structures. The characteristic peak at 20° indicate the formation of eumelanin [15]. Furthermore, there is a slightly shift conjugated with a remarkably decreasing in the intensity of this peak for all the co-doped samples which suggests that metals ions are linked to the eumelanin. Further, no new peaks of Fe, Zn, or Cu appear in the XRD patterns, confirming that doped metal ions are well bonded to the eumelanin molecule.

Scherrer's equation was used to calculate the crystallite size:

$$\mathbf{D} = \frac{k.\lambda}{\beta \cos \theta}$$

Were D being the crystallite size, k is a constant which is taken as 0.9 for spherical particle, λ is the X-ray wavelength (0.15406 nm), β is the full width at half maximum of the peak in radians, and θ know as diffraction angle or Bragg angle.

Average crystallite size of natural eumelanin is 1.93 nm and vary with the different metals. It's noted to be increasing to 3.73 nm and 2.01 nm after its co-doped with Fe and Cu ions respectively and decreased to 1.78 nm in the present of Zn ion. The significant increase in the crystallite size of the natural eumelanin powder that dopant with Fe ions (mel-Fe) is mostly due to the large size of Fe^{+3} ions, as it has a radius of approximately 63 p.m. XRD studies provide insights into the crystalline nature of melanin and how it is influenced by transition metal doping. Shifts in peak positions or the appearance of new peaks suggest modifications in the long-range ordering and crystallinity of the pigment.

Overall, the reduction of the amorphous structure of melanin by metal oxides is a complex process that involves electron transfer, oxidation-reduction reactions, and alterations to the molecular arrangement of melanin. The metal ions released from metal oxides during the reduction process can interact with melanin molecules. These interactions can result in the formation of coordination complexes or the induction of cross-linking between melanin molecules. Consequently, the amorphous structure of melanin can undergo further modifications.

2.4. Fourier transform infrared (FTIR) spectroscopic analysis

Fig. 3 shows the FTIR transmission spectra of pure eumelanin and the one doped with metals ions (mel-Zn, mel-Fe and, mel-Cu) in the 500 to 4000 cm^{-1} range. The catechol (O–H) group is present in the eumelanin's FTIR spectrum, which exhibits a distinctive broad band at 3406 cm^{-1}. The (C–H) stretching vibration is responsible for the bands at 2912 cm^{-1} and 2840 cm^{-1} [15]. Carboxylate (COO-) and/or aromatic (C═C) groups are thought to be the cause of the band at 1640 cm^{-1}. The stretching vibration (O–H) and (N–H) are responsible for the signals in the 2800-3800 cm^{-1} range [16]. The carboxylic acid and phenolic groups are related to the bands at 1040 cm^{-1} and 1528 cm^{-1} [18]. (C–H) vibrations are what cause the peak appears at 670–690 cm^{-1}. There are some changes in the FTIR spectrum when the metals ions Zn, Fe and Cu were bonded to the natural eumelanin. (O–H) group was from 3406 cm^{-1} toward a higher

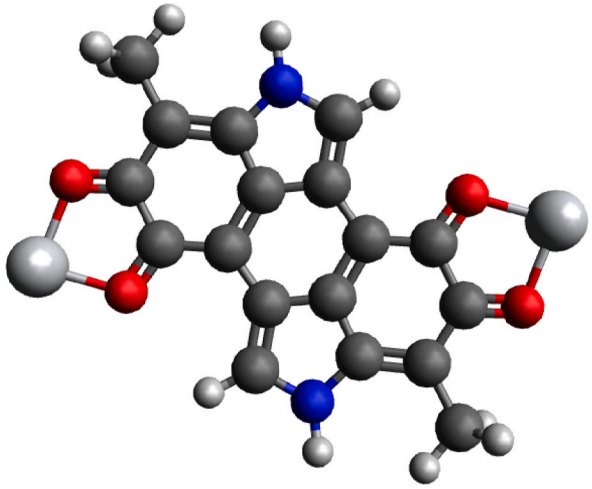

Fig. 4. Scheme of the molecular structure of eumelanin doped with metal ions (the dark gray are the carbon atoms, the red are the oxygen atoms, the blue are the nitrogen atoms, the white are the hydrogen atoms, and the light gray are the metal ions). (For interpretation of the references to color in this figure legend, the reader is referred to the Web version of this article.)

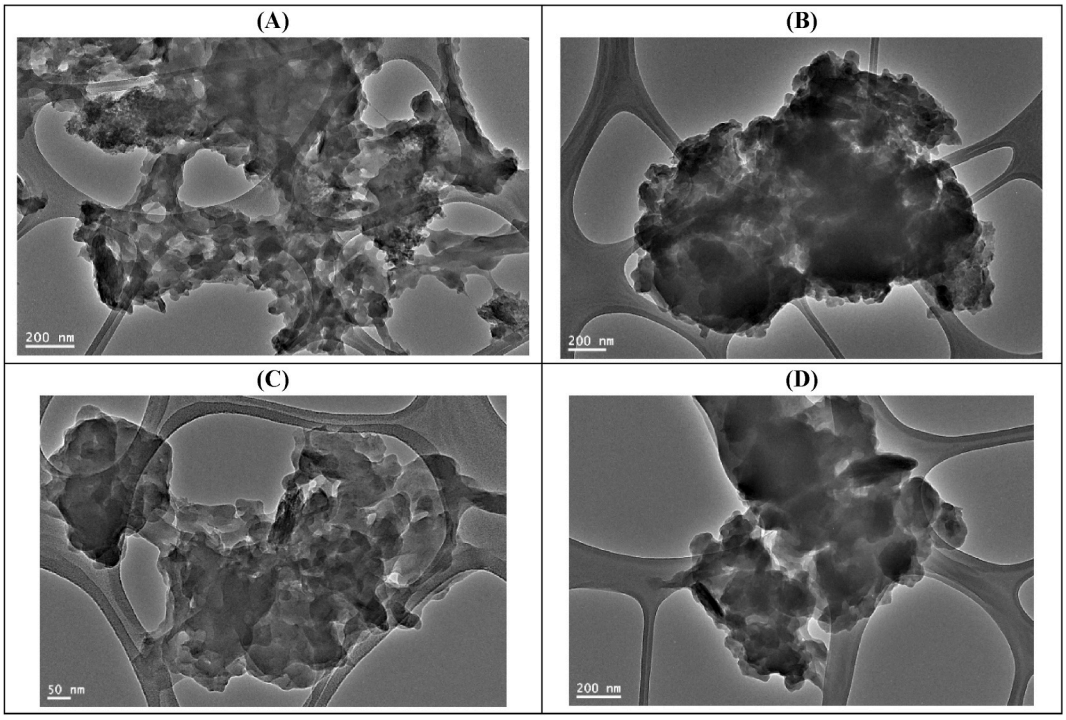

Fig. 5. TEM images of (A) pure natural eumelanin (B) Mel-Zn (C) Mel-Fe and, (D) Mel-Cu.

wavenumber. This suggests that the metal ions were attached the oxygen in the functional groups of eumelanin as shown in Fig. 4. There was a decreased in the peak intensity at 1640 cm^{-1} that associated with COO- with a slightly shift to 1638 cm-1. This indicates a connection between the metal ions and the ionized acid group. In the presence of Fe and Cu ions, the (C═C) or (COO-) stretching mode at the two bands at 2912 cm^{-1} and 2840 cm^{-1} are slightly shifted to 2926 cm^{-1} and 2856 cm^{-1}, respectively [11]. Furthermore, FTIR spectra show the Zn ions have no influence on the formation of eumelanin [18]. FTIR analysis reveals changes in the functional groups and bonding patterns of melanin after transition metal doping. This indicates alterations in the chemical composition and molecular structure of the pigment. Combined FTIR and XRD analysis offers a comprehensive understanding of the structural modifications occurring in melanin upon transition metal doping, enabling researchers to tailor its properties for various applications, including optoelectronics, bioengineering, and energy conversion.

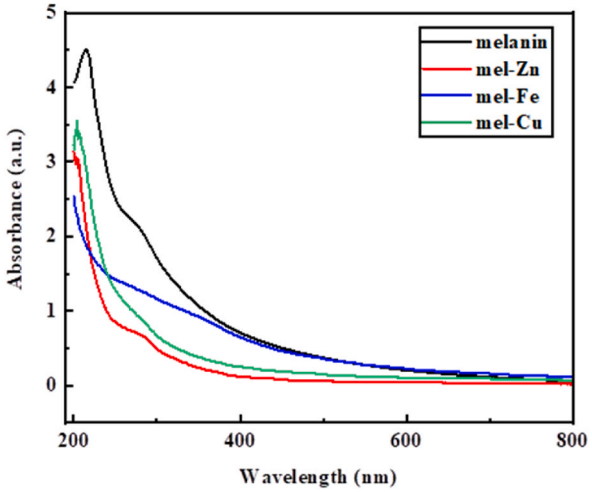

Fig. 6. The UV–vis absorbance spectra of pure natural eumelanin, mel-Zn, mel-Fe and mel-Cu.

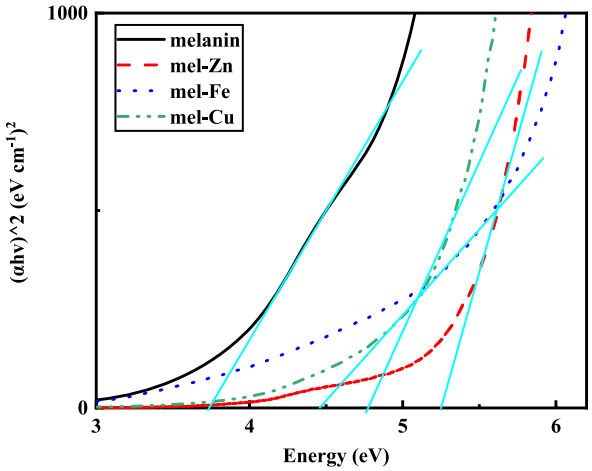

Fig. 7. Corresponding optical bandgap energy of eumelanin, mel-Zn, mel-Fe, and mel-Cu calculated by Tauc plots.

2.5. Transmission electron microscopy (TEM)

To characterize and describe the shape of the pure and co-doped natural eumelanin nanoparticles, transmission electron microscopy (TEM) was used. As seen in Fig. 5(A,B,C,D), natural eumelanin granules showed a spherical shape made from aggregates that are grouped together in amorphous organization, which is consistent with the findings from earlier studies [17,18]. The layers of pure natural eumelanin were damaged by the presence of metal ions (see Fig. 5(B-D)) and exist as many aggregates agglomerated together [3].

2.6. Optical properties

At room temperature, the optical absorption spectrum from 200 to 800 nm for eumelanin, mel-Zn, mel-Fe, and mel-Cu were examined, as shown in Fig. 6. The black color of eumelanin is a prove of their effective light absorbance behavior, which cover a wide range of UV and Visible region. After we doped metal ions with eumelanin, we see a loss of absorbance approximately to half in the UV range and remains primarily the same in the visible range in the present of Fe ions. On the same time, the absorption spectrum decreases dramatically when the eumelanin doped with Zn and Cu ions. This loss caused by the high concentration of water in the co-doped solution.

The following Tauc equation was used to determine the band gap energy (E_g) [18].

$$\alpha h\nu = K\left(h\nu - E_g\right)^n$$

Table 1
Optical parameters of pure natural eumelanin, mel-Zn, mel-Fe and mel-Cu.

Sample	UV radiation dose	Direct Bandgap (eV)	Urbach energy (eV)	Sample	UV radiation dose	Direct Bandgap (eV)	Urbach energy (eV)
Eumelanin	0 min	4.94	1.09	**Mel-Zn**	0 min	4.65	0.93
	240 min	4.89	1.12		240 min	4.57	0.81
	480 min	4.75	1.13		480 min	4.74	0.65
Mel-Fe	0 min	4.53	0.82	**Mel-Cu**	0 min	5.14	1.27
	240 min	5.01	0.72		240 min	5.25	1.06
	480 min	4.99	0.71		480 min	5.27	1.03

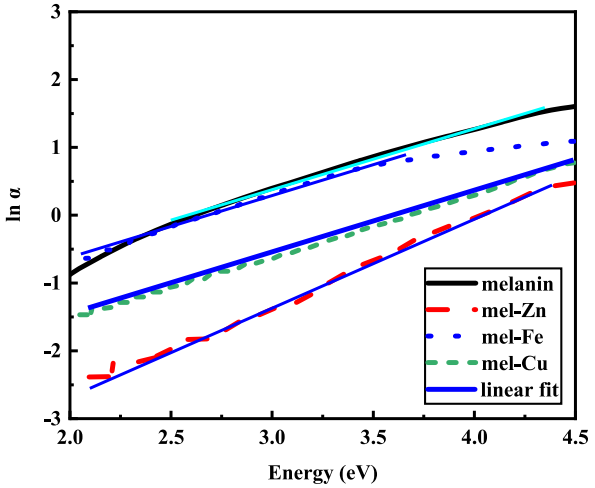

Fig. 8. Determination of Urbach energy for pure natural eumelanin, mel-Zn, mel-Fe and mel-Cu.

where h is Planck's constant, A is a constant, ν is the incident radiation frequency, n is equal to 2 for the direct band gap material and α is the absorption coefficient, which is calculated from the relation $\alpha = 2.303A/d$, where d is the pathlength of light and A is the measured absorbance. The band gap energy E_g can be estimated by plotting $(\alpha h\nu)^2$ versus energy $h\nu$ and extrapolating the linear portion of the plot to the x-axis. Fig. 7 shows that the band gap energies E_g of eumelanin, mel-Zn, mel-Fe and mel-Cu in Table 1. The energy band gap of eumelanin doped with metal ions significantly increase, especially in the present of Fe ions. This behavior can be explained by the bound of metal ions to oxygens in the functional groups of eumelanin. for instance, semiquinone groups, which can serve as potential sites for heavy metal accommodation such as Fe. In contrast, the catalyzing Fenton reactions resulted from the strong association of eumelanin with heavy metal ions such as iron and copper. This behavior can cause cell damage, while melanosomes work to trap them and prevent reducing and protecting cells from oxidative stress.

Urbach energy have been calculated as seen in Fig. 8 and (listed in Table 1). Urbach energy describe the cavity exponential broadening of absorption edge which related to the thermal and disorder structural model of semiconductor either amorphas (as eumelanin) or crystalline (as titanium dioxide). According to this concept, the Urbach energy is determined by exponential of an empirical optical gap, which is defined according to the following relation known as Urbach rule [19]:

$$\alpha = \alpha_0 \exp\left(\frac{h\upsilon}{E_u}\right)$$

where α is the absorption coefficient, α_0 is characteristic parameter depend on material, $h\upsilon$ is the incident photon energy and E_u is Urbach energy. Collectively, these observations led us to investigate the possibility that eumelanin doped with Fe, Cu and Zn may also participate in regulation of the pigmentation response to UV. In this study, we have resorted to calculating the Urbach energy [20], which is a description of the width of the defect bands formed in the energy gap of a material, at the edge of the equivalence band and the conduction band of the material, so it is known as the Urbach tail. The variation of the Urbach energy values can explained by the decrease or increase of the structural disorder and the improvement of the eumelanin monomers which is due in this case to the incorporation of the metal ion in the structure of resulted nanostructures [4]. In other words, the photosynthetic behavior of eumelanin with the presence of transition metals, which is evident in the absorption results after extended periods of time, shows an increase in the value of the energy gap with the passage of time in the presence of ultraviolet radiation. This means: A larger bandgap means that more energy is required to excite an electron from the valence band to the conduction band and hence light of a higher frequency and lower wavelength would be absorbed. This is exactly what happens with ultraviolet rays after the eumelanin doped with transition metals (Fe, Co and Zn). Interestingly, there were also increase in the Urbach energy is due to increasing irradiation time. This increase indicates: the degree of the absorption edge smearing and in crystalline lattice disordering enhancement of eumelanin as summarized

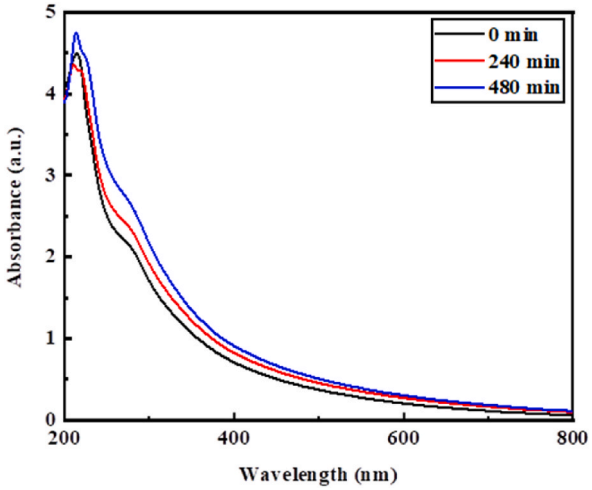

Fig. 9. The UV–Vis absorbance spectrum of pure natural eumelanin before and after increases the UV irradiation dose (The key to UV irradiation time are shown in the figure).

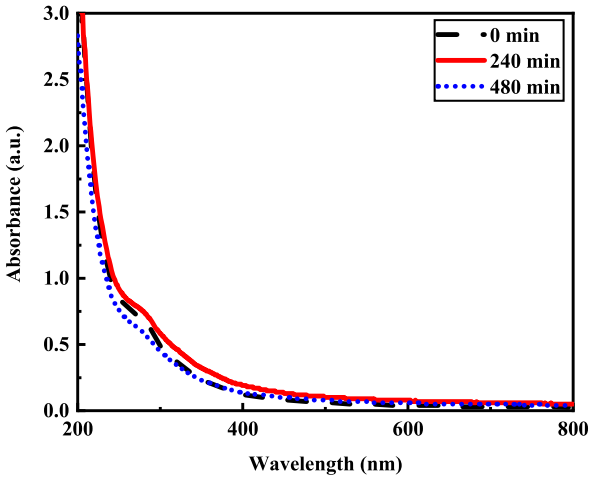

Fig. 10. The UV–Vis absorbance spectrum of mel-Zn before and after increases the UV irradiation dose (The key to UV irradiation time are shown in the figure).

in Table 1.

Fig. 9 shows the effect of UV-irradiation applied for 240 and 480 min to the pure natural eumelanin. It is notable that increasing the UV-irradiation dose resulting in an increase in the absorbance at the UV and visible region. The reason behind this is that UV-irradiation can causes certain chemical changes within eumelanin molecules such as the formation of new bonds between chromophores and increase the number of conjugated double bonds in the eumelanin structure which allows them to absorb lighter and increase the absorbance capability of the molecule and may shifts the peak of UV–vis absorbance spectrum little to higher wavelength [7]. As a result, the higher absorbance capability of the eumelanin aids in UV protection, helping to minimize damage to the cells. Moreover, the absorbance spectrum of eumelanin doped with Zn ions (Fig. 10) increases in the UV region after exposed to UV-irradiation due to the formation of new bonds between the Zn and eumelanin molecules. As UV-irradiation dose is increased, the bonds become stronger, which results in a decrease in the absorbance spectrum. This is because the bonds are now absorbing more UV light, reducing the amount of light that is available to be absorbed by the mel-Zn. On the other hand, when eumelanin doped with Fe the absorbent decrease after exposed to the UV radiation especially in the ultraviolet shortwave (UVC) region as shown in Fig. 11. This is due to Fe ion's high ability to absorb light, as is well known [21,22].When eumelanin doped with Cu, we notice a unique behaviour in the absorption spectrum (see Fig. 12), as the absorption decrease with increasing the UV-irradiation period in the shortwave (UVC) and middle-wave (UVB) ultraviolet region and increase in the longwave (UVA) ultraviolet and visible light region. This is likely due to good absorption property of UVA and visible light for copper ions [22].

We utilized density functional theory (DFT) to better understand the electronic structure and optical properties of the basic monomer in melanin from a theoretical standpoint. The DHICA monomer predominates in natural melanin, unlike the previously

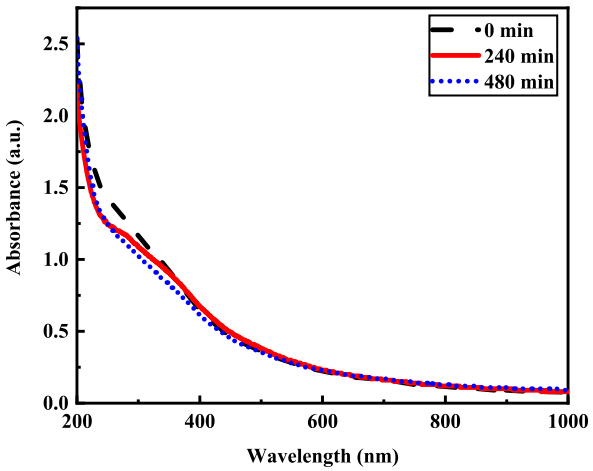

Fig. 11. The UV–Vis absorbance spectrum of mel-Fe before and after increases the UV irradiation dose (The key to UV irradiation time are shown in the figure).

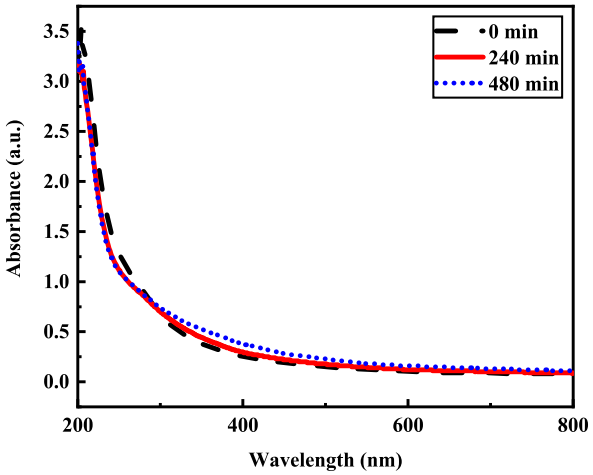

Fig. 12. The UV–Vis absorbance spectrum of mel-Cu before and after increases the UV irradiation dose (The key to UV irradiation time are shown in the figure).

studied DHI monomer(11). Fig. 13 shows the total density of states curves for DHICA eumelanin in the energy region after doping with Fe, Zn and Cu ions as shown in Fig. 13(A,B,C) respectively. The total density of states of the spin-polarized channels exhibit a symmetrical behavior for the Cu-DHICA and Zn-DHICA systems. In contrast, an asymmetrical behavior is seen for the Fe-DHICA system. Generally, the total density of states of the two spin channels is almost completely occupied in the energy region below the Fermi level, indicating that the Cu-DHICA and Zn-DHICA systems are semiconductors. However, the Fe-DHI system demonstrates half-metallic behavior.

The dielectric constant can be used to examine other significant optical properties. These optical characteristics may be computed using dielectric constants derived from DFT theory. To calculate the dielectric function, we used the Kohn-Sham formula of energy eigenvalues. According to the dynamical dielectric formula, which is represented as:

$$\boldsymbol{\varepsilon}(\boldsymbol{\omega}) = \boldsymbol{\varepsilon}_{\mathrm{RE}}(\boldsymbol{\omega}) \pm i\boldsymbol{\varepsilon}_{\mathrm{IMG}}(\boldsymbol{\omega})$$

The imaginary part $\boldsymbol{\varepsilon}_2(\boldsymbol{\omega})$ shows the probability of photon absorption and is calculated as follows. by Krong-Kramers relation, we can calculate the real part $\boldsymbol{\varepsilon}_{\mathrm{RE}}(\boldsymbol{\omega})$ from the imaginary part $\boldsymbol{\varepsilon}_{\mathrm{IMG}}(\boldsymbol{\omega})$ [21].

$$\boldsymbol{\varepsilon}_{\mathrm{IMG}}(\boldsymbol{\omega}) = \frac{\boldsymbol{e^2 e\hbar^2}}{\boldsymbol{\pi e m^2 e\omega^2}} \sum |\boldsymbol{\psi}_C|\hat{\boldsymbol{e}}.\vec{\boldsymbol{m}}|\boldsymbol{\psi}_V|^2 \boldsymbol{\delta}(\boldsymbol{E}_C - \boldsymbol{E}_V - \hbar\boldsymbol{\omega})$$

Where; ω is the frequency, ψ_C, ψ_V are the wave function of conduction and valence bands, respectively and $\vec{m}$ is the momentum element and E_C and E_V are the eigen

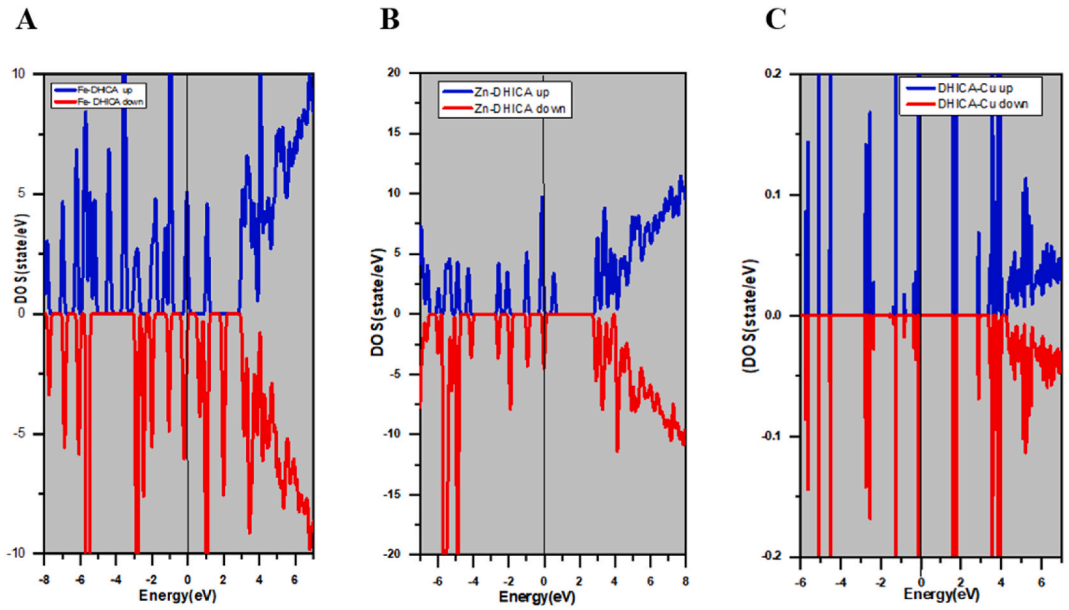

Fig. 13. Total Density of state of eumelanin monomer (DHICA) doped with Fe(A),Zn (B) and Cu(C) ions.

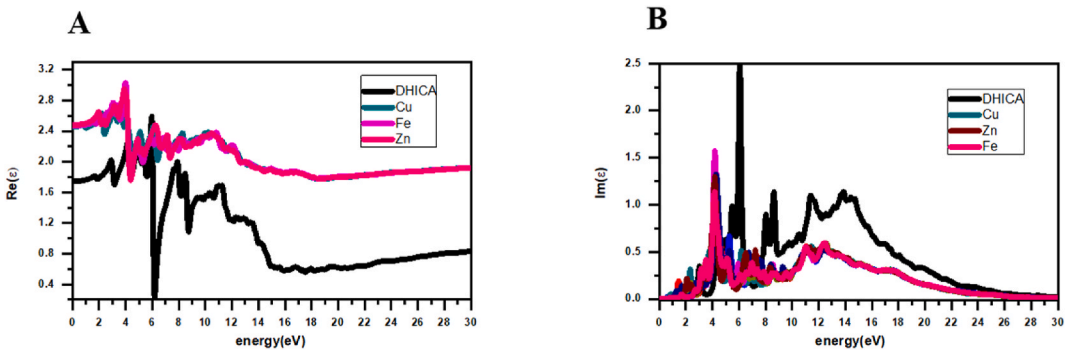

Fig. 14. Real (A) and Imaginary dielectric (B) calculated for DHICA doped with Fe,Zn and Cu ions.

The optical dielectric properties of DHICA were then investigated after doping with iron, copper, and zinc ions. Fig. 14-A shows the real (ε_{RE}) and Fig. 14-B shows imaginary (ε_{IMG}) parts of the dielectric function. The primary peaks are centered within approximate photon energy ranges. The real part (ε_{RE}) illustrates the polarization of matter when light interact with the material.The imaginary part (ε_{IMG}) indicates where photon absorption by the DHICA monomer is most probable. The results demonstrate that in the cases of iron and Zinc doping, the primary absorption peak appeared around 4.3eV and 4.6eV. copper doping produced a weaker reaction, with absorption peaked at a lower photon energy. In summary, DFT enabled calculation of the dielectric function and prediction of key optical characteristics like absorption spectra for the DHICA monomer system with different transition metal ion dopants.

3. Conclusion

In conclusion, this work significantly contributes to our understanding of the optical properties of eumelanin through the investigation of pure and doped eumelanin with three transition metals(Fe,Cu and Zn) under varying exposing durations of ultraviolet radiation. The results indicate a notable correlation between increased exposure to radiation and a decrease in the energy gap of doped eumelanin. The application of density functional theory further deepened our comprehension of the electronic structures of melanin. Moreover, the study elucidated the optical and structural changes that arise from the introduction of transition metals, resulting in enhanced properties resembling semiconductors within a spin-polarized system. The significance of this research lies in its contribution to our understanding of the biological characteristics of melanin, particularly in relation to diseases associated with an elevated proportion of melanin and minerals within living cells.

CRediT authorship contribution statement

Nawal Madkhali: Writing – review & editing, Methodology, Investigation. **Saja Algessair:** Writing – original draft, Software, Methodology, Investigation.

Declaration of competing interest

The authors declare that they have no known competing financial interests or personal relationships that could have appeared to influence the work reported in this paper.

References

[1] F. Solano, F. Solano, Melanins: skin pigments and much more—types, structural models, biological functions, and formation routes, New J Sci 2014 (2014) 1–28, https://doi.org/10.1155/2014/498276.

[2] A. Napolitano, A. Pezzella, G. Prota, R. Seraglia, P. Traldi, Structural analysis of synthetic melanins from 5,6-dihydroxyindole by matrix-assisted laser desorption ionization mass spectrometry, Rapid Commun. Mass Spectrom. 10 (4) (1996) 468–472.

[3] N. Madkhali, H.R. Alqahtani, S. Al-Terary, A. Laref, A. Hassib, Control of optical absorption and fluorescence spectroscopies of natural melanin at different solution concentrations, Opt. Quant. Electron. (2019), https://doi.org/10.1007/s11082-019-1936-3.

[4] Y. Liu, J.D. Simon, Metal-ion interactions and the structural organization of Sepia eumelanin, Pigm. Cell Res. 18 (1) (2005) 42–48, https://doi.org/10.1111/j.1600-0749.2004.00197.x.

[5] M. Ambrico, et al., From commercial tyrosine polymers to a tailored polydopamine platform: concepts, issues and challenges en route to melanin-based bioelectronics, J. Mater. Chem. C 3 (2015) 6413–6423, https://doi.org/10.1039/C5TC00570A.

[6] P.P.A.P. Riley, Melanin, Int. J. Biochem. Cell Biol. 29 (Ii) (1997) 1235–1239, https://doi.org/10.1016/S1357-2725(97)00013-7.

[7] M.L. Tran, B.J. Powell, P. Meredith, Chemical and structural disorder in eumelanins: a possible explanation for broadband absorbance, Biophys. J. 90 (3) (2006) 743–752, https://doi.org/10.1529/biophysj.105.069096.

[8] M.G. Bridelli, P.R. Crippa, Theoretical analysis of the adsorption of metal ions to the surface of melanin particles, Adsorption 14 (1) (2008) 101–109, https://doi.org/10.1007/s10450-007-9059-8.

[9] M. Okazaki, K. Kuwata, Y. Miki, S. Shiga, T. Shiga, Electron spin relaxation of synthetic melanin and melanin-containing human tissues as studied by electron spin echo and electron spin resonance, Arch. Biochem. Biophys. 242 (1) (1985) 197–205.

[10] Y. Liu, L. Hong, V.R. Kempf, K. Wakamatsu, S. Ito, J.D. Simon, Ion-exchange and adsorption of Fe(III) by Sepia melanin, Pigm. Cell Res. 17 (3) (2004) 262–269, https://doi.org/10.1111/j.1600-0749.2004.00140.x.

[11] C. Sarzanini, E. Mentasti, O. Abollino, M. Fasano, S. Aime, Metal-ion content in sepia-officinalis melanin, Mar. Chem. 39 (4) (1992) 243–250 [Online]. Available: <Go to ISI>://A1992JT55300001.

[12] X. Tan, et al., Epidermal growth factor receptor: a novel target of the Wnt/beta-catenin pathway in liver, Gastroenterology 129 (1) (2005) 285–302.

[13] W. Osak, K. Tkacz-??miech, M. Elbanowski, J. S??awi??ski, "Dielectric and electric properties of synthetic melanin: the effect of europium ions,", J. Biol. Phys. 21 (1) (1995) 51–65, https://doi.org/10.1007/BF00701009.

[14] I. Marcovici, et al., Melanin and melanin-functionalized nanoparticles as promising tools in cancer research—a review, Cancers 14 (7) (2022), https://doi.org/10.3390/cancers14071838.

[15] E.-O. A, et al., Herbal Melanin Modulates PGE2 and IL-6 Gastroprotective Markers through COX-2 and TLR4 Signaling in the Gastric Cancer Cell Line AGS, 2022, https://doi.org/10.21203/RS.3.RS-1597711/V1.

[16] A. El-Obeid, A. Hassib, F. Pontén, B. Westermark, Effect of herbal melanin on IL-8: a possible role of Toll-like receptor 4 (TLR4), Biochem. Biophys. Res. Commun. 344 (4) (2006) 1200–1206, https://doi.org/10.1016/j.bbrc.2006.04.035.

[17] N. Madkhali, H.R. Alqahtani, S. Al-Terary, A. Laref, A. Haseeb, The doping effect of Fe, Cu and Zn ions on the structural and electrochemical properties and the thermostability of natural melanin extracted from Nigella sativa L, J. Mol. Liq. (2019), https://doi.org/10.1016/j.molliq.2019.04.063.

[18] Shimadzu Corporation, Measurements of band gap in compound semiconductors - band gap determination from diffuse reflectance spectra -, Measurement (1800).

[19] F. Urbach, The long-wavelength edge of photographic sensitivity and of the electronic absorption of solids, Phys. Rev. 92 (5) (1953) 1324, https://doi.org/10.1103/PhysRev.92.1324.

[20] B.A. El-Badry, N. Madkhali, A.M. Deghady, Influence of eumelanin and gamma irradiation on ZnO nanocomposite properties, Radiat. Phys. Chem. 191 (2022) 109845, https://doi.org/10.1016/J.RADPHYSCHEM.2021.109845.

[21] D.S. Sholl, J.A. Steckel, Density functional theory: a practical introduction, Density Functional Theory: A Practical Introduction (2009) 1–238, https://doi.org/10.1002/9780470447710.